Jurnal Tribologi 39 (2023) 1-16

MYTRIBOS Malaysian Tribology Society

Jurnal Tribologi

Website : jurnaltribologi.mytribos.org e-issn: 2289-7232

Applied normal load and printing layer thickness relationship on the tribological properties of novel 3D-printed PLA-PCU polymer blend

Shanahs Shaharuddin [1], Mohd Fadzli Bin Abdollah [1,2*], Hilmi Amiruddin [1,2], Shahira Liza Kamis [3], Faiz Redza Ramli [1,2]

[1] Faculty of Mechanical Technology and Engineering, Universiti Teknikal Malaysia Melaka, Hang Tuah Jaya, 76100 Durian Tunggal, Melaka, MALAYSIA.
[2] Centre for Advanced Research on Energy, Universiti Teknikal Malaysia Melaka, Hang Tuah Jaya, 76100 Durian Tunggal, Melaka, MALAYSIA.
[3] Malaysia-Japan International Institute of Technology, Universiti Teknologi Malaysia, Jalan Sultan Yahya Petra, Kampung Datuk Keramat, 54100 Kuala Lumpur, MALAYSIA.
*Corresponding author: mohdfadzli@utem.edu.my

KEYWORDS

3D print
Polymer
Coefficient of friction
Wear

ABSTRACT

This study aims to investigate the tribological properties of a new additively manufactured polymer blend made of polycarbonate-urethane (PCU) and poly(lactic acid) (PLA) under lubricated conditions. A ball-on-disc tribometer was utilised to conduct tribological testing. The findings found that the PLA-PCU polymer blend has a lower elastic modulus and hardness than pure PLA. However, there is no substantial difference in tribological properties between the two materials. Regardless of polymer blend composition, the coefficient of friction (COF) and wear rate of 3D-printed materials decrease with increasing printing layer thickness and applied normal load. The wear mechanisms are dominated by plastic deformation. As the applied normal load increases, the deformation regime transitions from abrasive wear and surface microcracks to compaction and layer detachment.

Received 15 May 2023; received in revised form 21 August 2023; accepted 6 October 2023.
To cite this article: Shaharudin et al., (2023). Applied normal load and printing layer thickness relationship on the tribological properties of novel 3D-printed PLA-PCU polymer blend. Jurnal Tribologi 39, pp.1-16.

1.0 INTRODUCTION

The idea of developing a blend of two or more polymers is not to drastically alter the properties of the components, but rather to maximise the performance of the blend by a physical technique that may or may not require a compatibilizer (Yu et al. 2006). There are two conventional methods for producing polymer blends (Toh et al., 2021): solvent blending, which requires dissolving a polymer and filler mixture in a co-solvent, followed by evaporating the solvent. The other method is melting blending, which involves blending and shearing molten polymer and filler. However, melt blending was used in this study, in which both polymers were heated and mixed in a molten state using a twin-screw extruder due to the high shear elements present, resulting in a more homogeneous combination (Martin, 2016).

Poly (lactic acid) (PLA) and its composites have been widely used in clinical applications, particularly for articular cartilage (DeStefano et al., 2020). This material is biocompatible, durable, and resistant to wear. The current formative manufacturing-created artificial cartilage implant is incapable of sustaining joint lubrication via the weeping mechanism due to a lack of porosity. PLA also has a higher elastic modulus than articular cartilage and is subject to mechanical restriction (Saini et al., 2016). Polycarbonate-urethane (PCU) is a promising material for artificial articular cartilage because its elastic modulus is comparable to that of articular cartilage (Beckmann et al., 2016 & Kanca et al., 2018). PCU is employed in many implants, including orthopaedic prostheses, due to its mechanical qualities and biocompatibility (Beckmann et al., 2016), and demonstrates favourable wear and friction performance (Kanca et al., 2018).

Fused filament fabrication (FFF) is an additive manufacturing technology that was developed to reduce procedure time and steps. It is also less expensive, faster, and less complicated to run than the other processes. Despite this, FFF samples exhibit poor mechanical qualities and rougher surfaces (Rouf et al., 2022). Although 3D printing technology is utilised to fabricate PCU-based products, the manufacturing process requires the use of a high-end 3D printer with specific nozzles or techniques because of the soft polymer properties (Miler et al., 2017). A 3D printed blend of PLA and other biodegradable and biocompatibility polymers such as PCU, could potentially address this issue.

As a result of the above discussion, the purpose of this study is to investigate the tribological properties of a 3D-printed polymer blend made up of 10 wt.% PCU and 90 wt.% PLA. The outcomes were compared to those of pure 3D-printed PLA. The discussion focuses on the relationship between applied normal load and printing layer thickness on the tribological properties of 3D-printed PLA-PCU under lubricated conditions.

2.0 METHODOLOGY

2.1 Polymer Blend Filament Preparation

Two batches of polymer blends were prepared for 3D printing filament preparation: 100 wt.% PLA (100PLA) and 90 wt.% PLA with 10% PCU (90PLA-10PCU). The optimal mixture composition is based on a previous study (Kazim et al., 2022). The batches were mixed in an internal mixer before being extruded using a twin-screw extruder into 1.75±0.17mm diameter filament.

2.2 3D-Printed Polymer Blend Fabrication

The fabrication of 3D-printed samples begins with the design of the sample in SolidWorks with dimensions of 35mm x 35mm x 3mm. The filament was then fed into a FlashForge 3D printer (Fused filament fabrication (FFF) technique) with the optimal printing parameters (Table 1). The printing parameters are from a previous study (Kazim et al., 2022). Figure 1 shows 3D-printed PLA-PCU and 3D-printed PLA samples.

Table 1: Optimal printing parameters.

Printing Parameters	**Value**
Layer thickness (mm)	0.10, 0.12, 0.14, 0.16
Nozzle temperature (°C)	195
Printing bed temperature (°C)	50
Nozzle speed (mm/s)	15
Printing infill (%)	100
Printing pattern	Hexagon

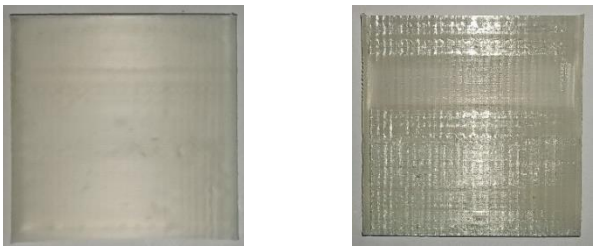

(a) (b)

Figure 1: (a) 3D-printed PLA-PCU and (b) 3D-printed PLA samples.

2.3 Tribology and Materials Properties Tests

Tribological testing was performed in accordance with ASTM G99, 2017 using a ball-on-disc tribometer (Figure 2). A sample was slid against a 12 mm diameter chrome steel ball (with a hardness of 7.45 GPa, average surface roughness of 0.022 μm, and Young's modulus of 210 GPa) and continuously titrated with Ringer solution. The Ringer solution 1/4 strength tablets was supplied by Sigma-Aldrich and utilised to simulate body fluid (Kazerooni et al., 2011). One tablet of Ringer solution was dissolved in 500 ml of deionised water. The average dynamic viscosity of the Ringer solution is 1.14 mPa.s. Table 2 shows the composition of Ringer solution, while Table 3 shows the tribological testing parameters according to ASTM G99. The sample material and steel ball were cleaned with acetone prior to the test. This five-minute pre-cleaning was carried out to remove contaminants. Coefficient of friction (COF) and wear rate are calculated using Eqns. (1) and (2), respectively.

$$\mathrm{COF}=\frac{F}{W} \tag{1}$$

$$k = \frac{V_{loss}}{WL} \quad (2)$$

Where, COF is the ratio of friction force (F) and the applied normal load (W); both measured in Newton's. Wear rate k (mm^3/Nm) is calculated using volume loss V_{loss} (mm^3), sliding distance L (m).

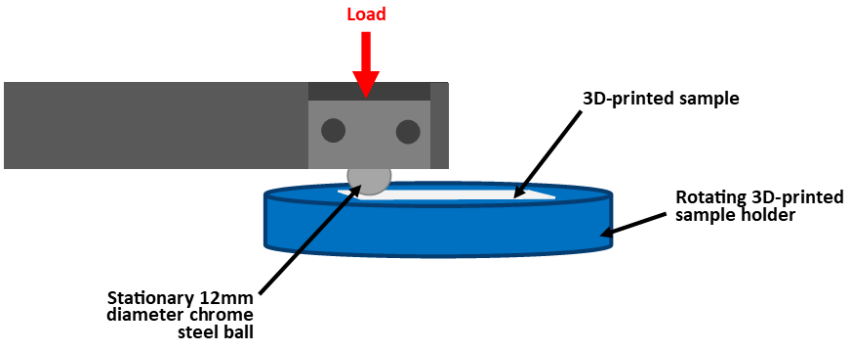

Figure 2: Schematic diagram of a ball-on-disc tribometer.

Table 2: Composition of Ringer solution supplied by Sigma-Aldrich.

Parameters	**g/L**
Calcium chloride hexahydrate	0.120
Potassium chloride	0.105
Sodium bicarbonate	0.050
Sodium chloride	2.250

Table 3: Testing parameters for tribological testing.

Parameters	**Value**
Sliding speed (rpm)	200
Applied normal loads (N)	30, 50, 70
Sliding distance (m)	1000
Wear track diameter (mm)	20

The sample's hardness was tested with a Shore-D durometer. In order to measure the elastic modulus of the sample, only moulded PLA-PCU and PLA were employed. This is due to the variable value obtained for 3D-printed samples. A compression test on universal testing equipment was used to measure the elastic modulus of the samples.

Surface morphology and topography of the tested materials was observed using Scanning Electron Microscopy (SEM) and surface roughness tester, accordingly. Figure 3 shows the procedure for measuring surface roughness.

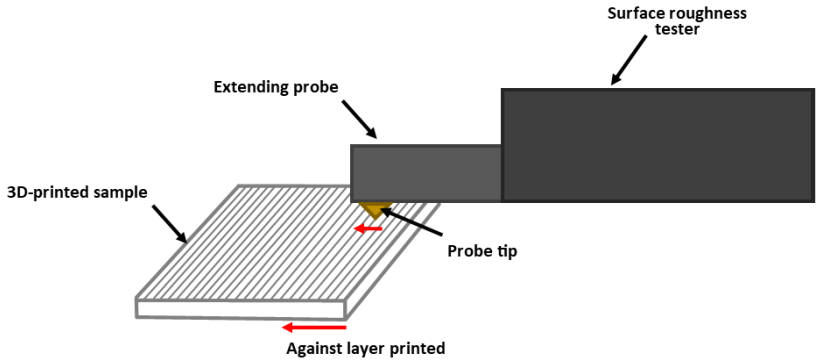

Figure 3: Schematic diagram of a surface roughness test.

The contact angle or wettability test was used to determine whether the polymer blend PLA-PCU has hydrophobic or hydrophilic characteristics. From Figure 4, the sample was positioned on the stage perpendicular to the microscope for the contact angle test, so that the ridges of the 3D-printed could be viewed against the microscope. Then, using an auto-pipette, Ringer's solution was cautiously dripped onto the sample at the edge closest to the microscope; this process was repeated at least ten times along the same edge of the sample, yielding an average angle. After taking photographs of the Ringer's droplet, the inner angle of the Ringer's droplet was determined using ImageJ, a measurement software.

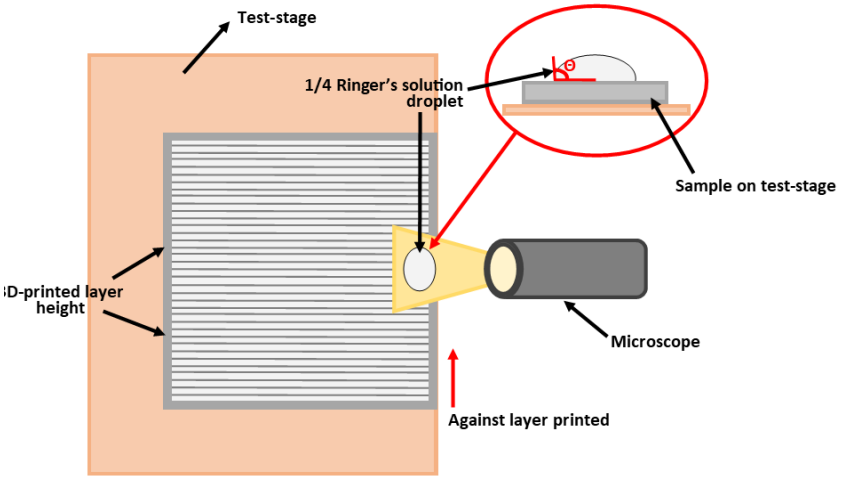

Figure 4: Schematic diagram of contact angle test.

3.0 RESULTS AND DISCUSSION

3.1 Friction and Wear Properties

The elastic modulus and hardness of the polymer blends are shown in Figure 5. Figure 6 shows the COF and wear rate for both 3D-printed PLA-PCU and 3D-printed PLA samples. Even though polymer blends (90PLA-10PCU) have lower elastic modulus and hardness than pure PLA, there is no significant effect in COF and wear rate between 3D-printed PLA-PCU and 3D-printed PLA because the data scattered randomly. This demonstrates that the incorporation of PCU in PLA served as a "bridge" to reduce PLA elasticity without affecting its tribological properties.

According to the contour map in Figures 7 and 8, the distribution of COF and wear rate of 3D-printed materials decrease with increasing applied normal load at a thicker printing layer, regardless of polymer blend composition. Surface roughness increased significantly with increasing printing layer thickness, as shown in Figure 9. This is consistent with Ayrilmis, 2018 and Liu et al., 2021. As the printing layer thickness increased, the outside profile of each layer got more rounded, and the contact area increased. As a result, the pressure distribution on the contact surface is smaller than that on a thinner printing layer, resulting in a lower COF and wear rate. This behaviour is in line with the friction adhesion theory, which states that the shear resistance during sliding depends on the relationship between the contact area and shear stress (Rabinowicz & Tanner, 1966).

The relationship between roughness and wettability was defined by Wenzel's theory, which stated that increasing surface roughness increases wettability induced by surface chemistry. Wettability is the ability of a liquid to spread over and establish contact with a solid surface. Increased wettability (decrease contact angle) indicates that the liquid can spread more freely across the surface, resulting in a greater contact area and better adhesion between the liquid and the solid. According to Ayrilmis, 2018, increasing the printing layer thickness increased the surface roughness and number of microholes on the surface of samples, resulting in more liquid absorption, this improved wettability. In other words, the wettability significantly increased with increasing printing layer thickness, as shown in Figure 10. Surprisingly, high wettability surfaces with higher roughness have lower COF values than smoother surfaces (Conradi et al., 2018).

The impact of surface roughness on debris formation is self-evident. Debris formation as a result of mechanical and contact fatigue stress promotes surface deformation in the contact area resulting in a lower COF and wear rate (Sinha & Briscoe, 2009). This mechanism will be discussed more in Section 3.2.

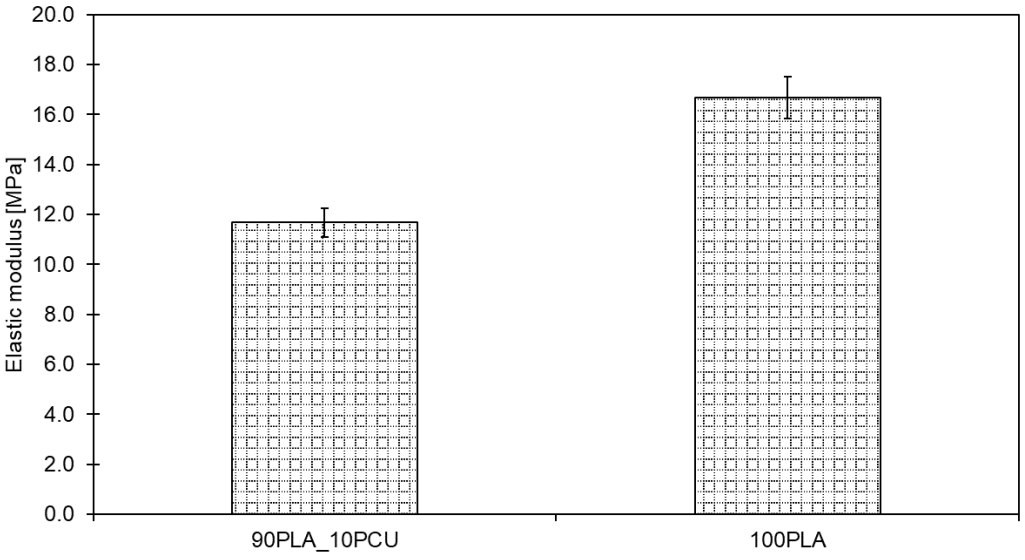

(a)

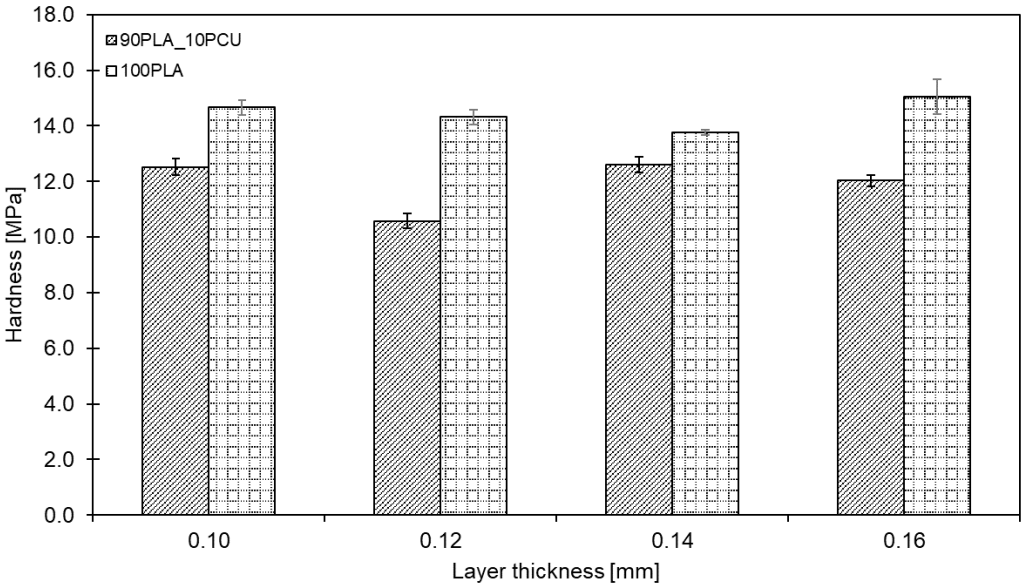

(b)

Figure 5: (a) Elastic modulus comparison for PLA-PCU polymer blend and pure PLA. (b) Hardness comparison of 3D-printed PLA-PCU and 3D-printed PLA at different printing layer thickness.

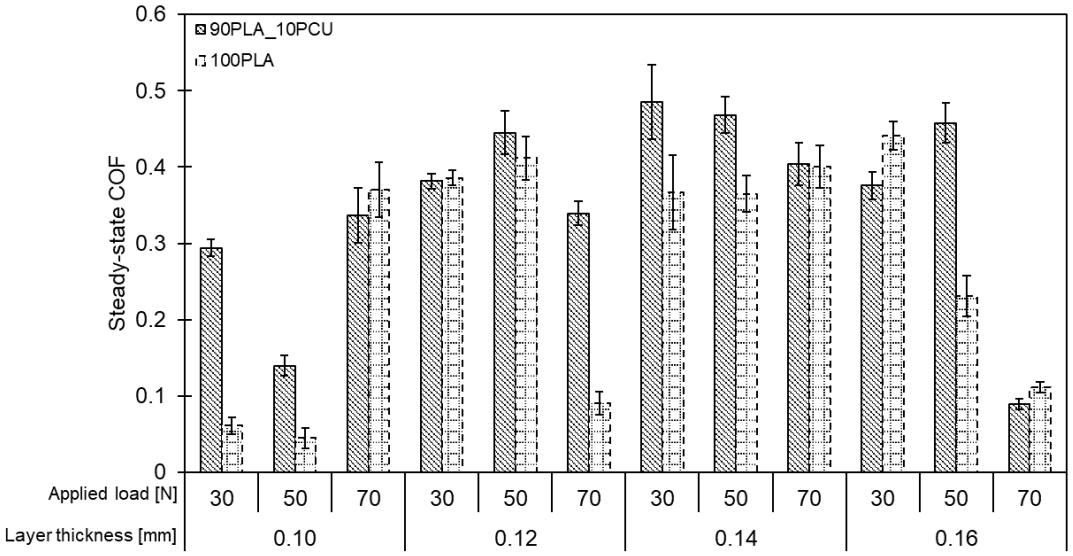

(a)

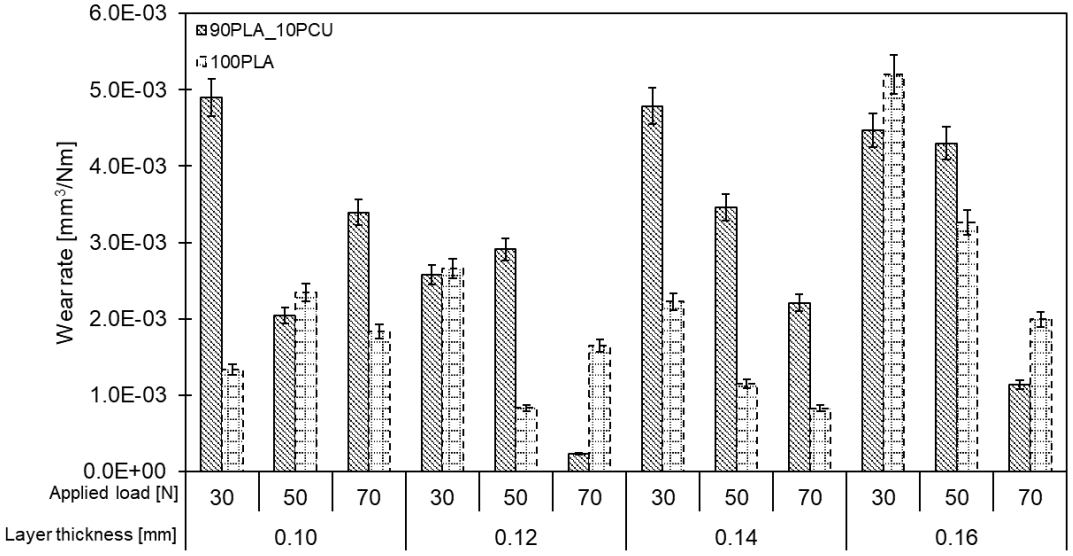

(b)

Figure 6: (a) Steady-state COF and (b) wear rate values for 3D-printed PLA-PCU and 3D-printed PLA.

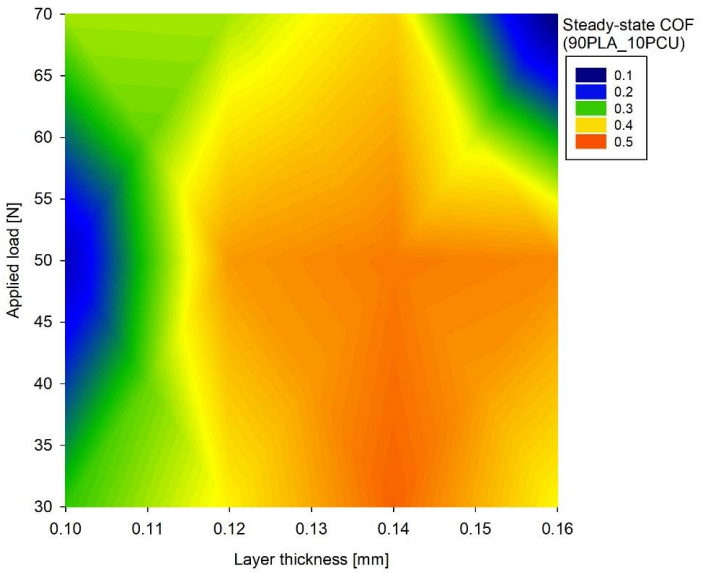

(a)

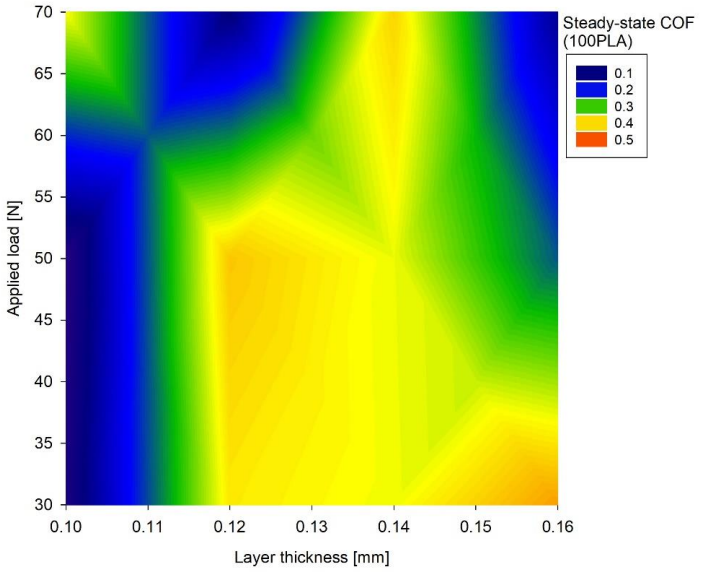

(b)

Figure 7: Relationship between the applied normal load and printing layer thickness on the steady-state COF of (a) 3D-printed PLA-PCU and (b) 3D-printed PLA.

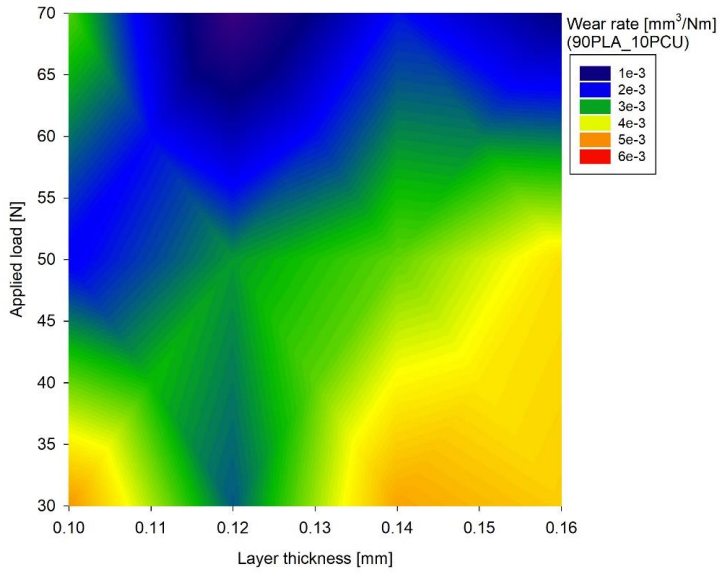

(a)

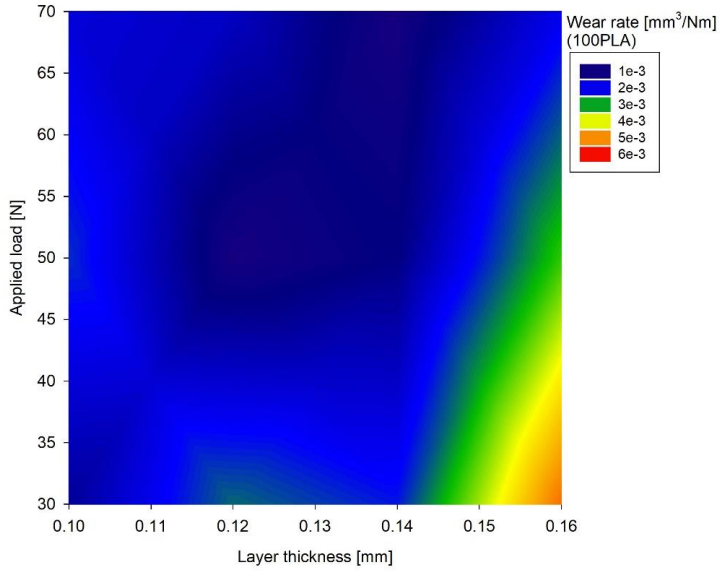

(b)

Figure 8: Relationship between the applied normal load and printing layer thickness on the wear rate of 3D-printed PLA-PCU and 3D-printed PLA.

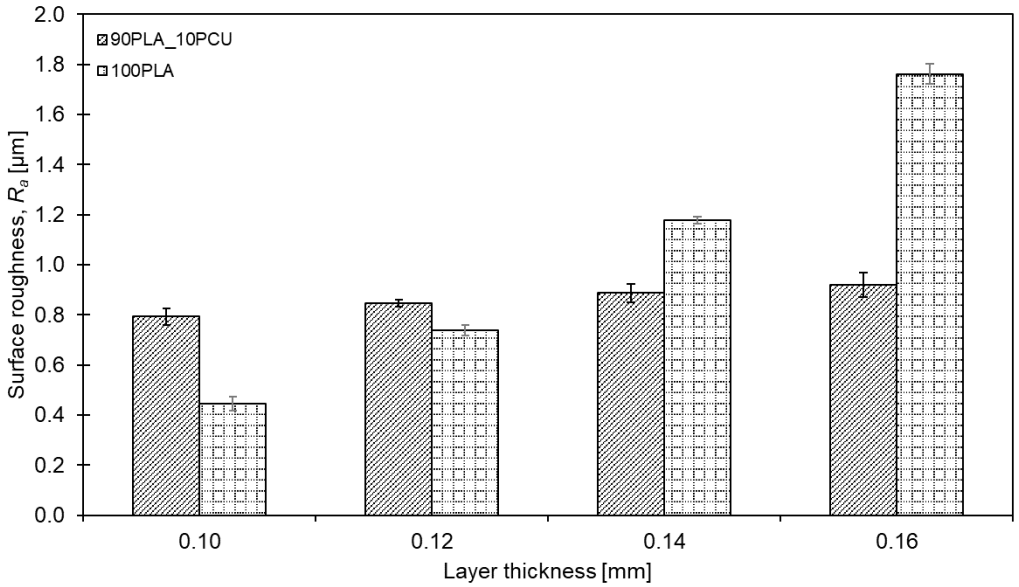

Figure 9: Surface roughness values for 3D-printed PLA-PCU and 3D-printed PLA at different printing layer thickness.

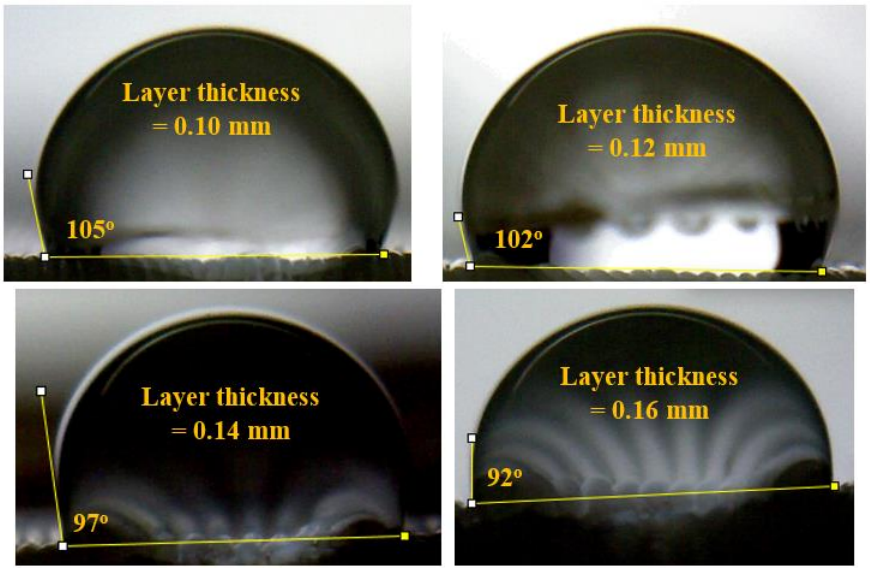

(a)

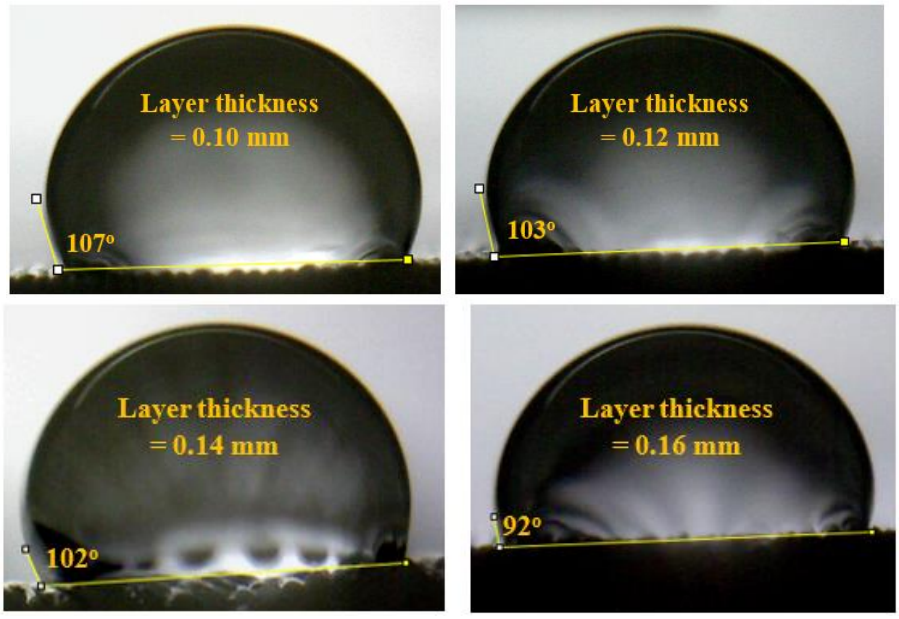

(b)

Figure 10: Effect of layer thickness on the surface wettability of (a) 3D-printed PLA-PCU and (b) 3D-printed PLA.

3.2 Wear Mechanisms

A comprehensive analysis to correlate friction and wear performance with wear mechanisms is performed to further understand the transient behaviour observed for the test samples at varying applied normal loads and printing layer thicknesses. Figures 7 and 8 show that the distribution of decreased COF and wear rate for both 3D-printed PLA-PCU and 3D-printed PLA is achieved with a higher applied normal load and a thicker printing layer. Figure 11 shows micrograph images of the worn surface showing the progression of asperity deformation with applied normal load at a thicker printing layer (0.16 mm). At higher applied normal loads, the most noticeable surface deformation is caused by the compaction of the overlapping raster layers. Dawoud et al., 2015 reported a similar deformation phenomenon using a polymer sample printed with the FFF technique under high load. Increasing the applied normal load from 30 to 70 N results in a transition from abrasive wear and surface microcracks to a mixed regime of compaction and layer detachment. Increasing load causes increased surface layer detachment as abrasive and adhesive damage increases. High contact loads and surface asperities ploughing cause the surface to deform plastically. The Schallamach pattern (Barquins, 1985) is a well-known abrasive pattern that promotes layer detachment and surface buckling. Asperity deformation promotes the formation of wear debris within the wear track, which works as a lubricating layer to control friction and wear at higher applied normal loads. Consequently, the formation of third body particles acts as a lubricant during wear.

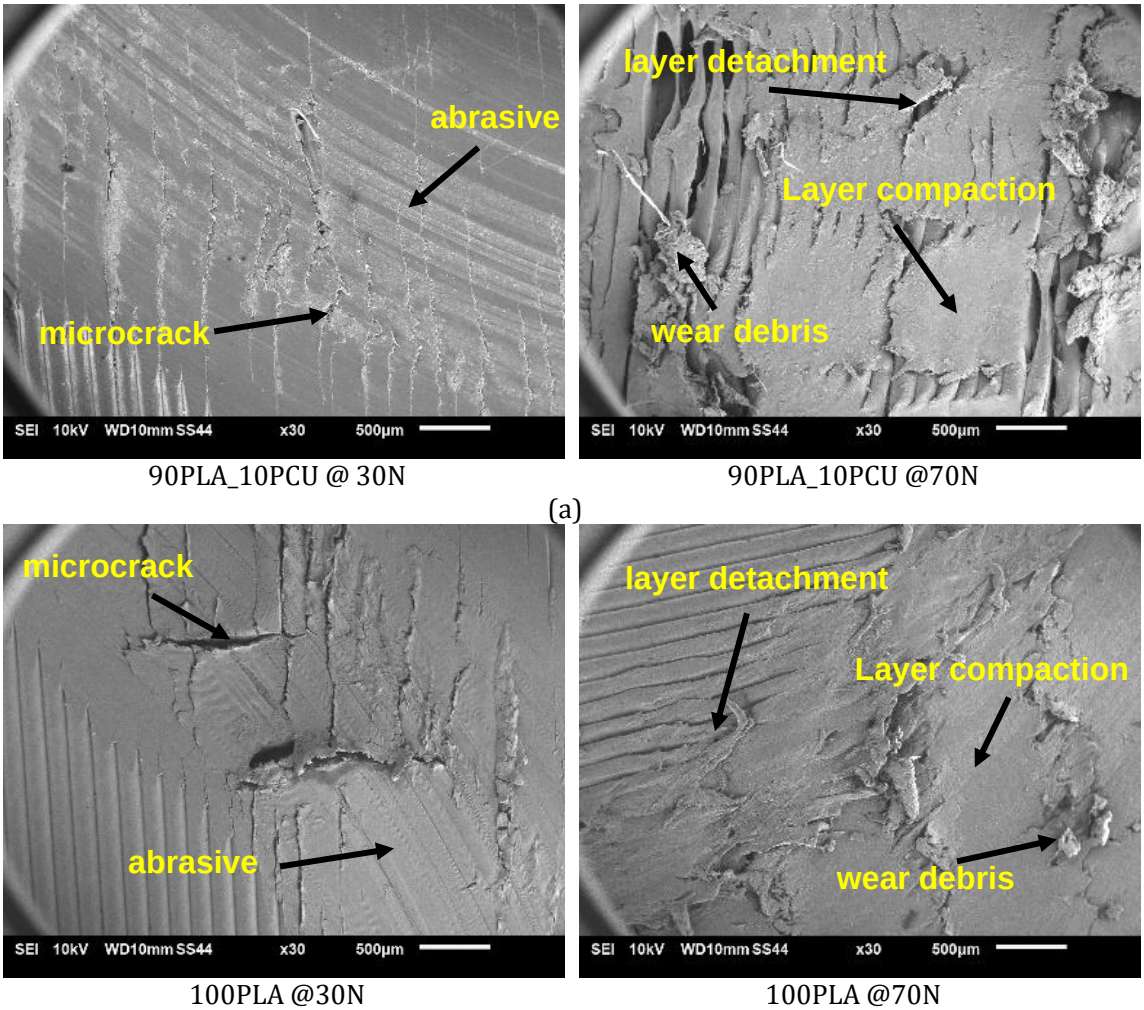

90PLA_10PCU @ 30N 90PLA_10PCU @70N

(a)

100PLA @30N 100PLA @70N

(b)

Figure 11: SEM images of (a) 3D-printed PLA-PCU and (b) 3D-printed PLA under low and high applied normal loads at 0.16mm printing layer thickness.

CONCLUSIONS

Although the PLA-PCU polymer blend has a lower elastic modulus and hardness than pure PLA, the COF and wear rate are not significantly different between the two materials. However, COF and wear rates of 3D-printed materials decrease with increasing printing layer thickness and applied normal load, regardless of polymer blend composition. Plastic deformation is the predominant wear mechanism. The deformation regime transitions from abrasive wear and surface microcracks to a mixed regime of compaction and layer detachment as the applied normal load increases. This study adds to the growing body of knowledge about the possible applications of a 3D-printed PLA-PCU polymer blend as artificial articular cartilage.

ACKNOWLEDGMENTS

This study is supported by a grant from Ministry of Higher Education Malaysia (Grant no.: FRGS/1/2020/TK0/UTEM/03/4). The authors gratefully acknowledge use of the services and facilities of the Universiti Teknikal Malaysia Melaka and Malaysia-Japan International Institute of Technology.

REFERENCES

ASTM G99 (2017) Standard Test Method for Wear Testing with a Pin-on-Disk Apparatus.

Ayrilmis, N. (2018). Effect of layer thickness on surface properties of 3D printed materials produced from wood flour/PLA filament. Polymer testing, 71, 163-166.

Barquins, M. (1985). Sliding friction of rubber and Schallamach waves—a review. Materials Science and Engineering, 73, 45-63.

Beckmann, A., Herren, C., Nicolini, L. F., Grevenstein, D., Oikonomidis, S., Kobbe, P., ... & Siewe, J. (2019). Biomechanical testing of a polycarbonate-urethane-based dynamic instrumentation system under physiological conditions. Clinical Biomechanics, 61, 112-119.

Conradi, M., Drnovšek, A., & Gregorčič, P. (2018). Wettability and friction control of a stainless steel surface by combining nanosecond laser texturing and adsorption of superhydrophobic nanosilica particles. Scientific reports, 8(1), 1-9.

Dawoud, M., Taha, I., & Ebeid, S. J. (2015). Effect of processing parameters and graphite content on the tribological behaviour of 3D printed acrylonitrile butadiene styrene: Einfluss von Prozessparametern und Graphitgehalt auf das tribologische Verhalten von 3D-Druck Acrylnitril-Butadien-Styrol Bauteilen. Materialwissenschaft und Werkstofftechnik, 46(12), 1185-1195.

DeStefano, V., Khan, S., & Tabada, A. (2020). Applications of PLA in modern medicine. Engineered Regeneration, 1, 76-87.

Kanca, Y., Milner, P., Dini, D., & Amis, A. A. (2018). Tribological evaluation of biomedical polycarbonate urethanes against articular cartilage. Journal of the Mechanical Behavior of Biomedical Materials, 82, 394-402.

Kazerooni, N. A., Bahrololoom, M. E., Shariat, M. H., Mahzoon, F., & Jozaghi, T. (2011). Effect of Ringer's solution on wear and friction of stainless steel 316L after plasma electrolytic nitrocarburising at low voltages. Journal of Materials Science & Technology, 27(10), 906-912.

Kazim, M. N. A., Abdollah, M. F. B., Amiruddin, H., Liza, S., Ramli, F. R., & Tunggal, D. (2022). Surface quality and absorption properties of polymeric composite (PLA-PCU) fabricated using 3D printing for articular cartilage application. Jurnal Tribologi, 35, 169-185.

Liu, Y., Bai, W., Cheng, X., Tian, J., Wei, D., Sun, Y., & Di, P. (2021). Effects of printing layer thickness on mechanical properties of 3D-printed custom trays. The Journal of Prosthetic Dentistry, 126(5), 671-e1.

Martin, C. (2016). Twin screw extruders as continuous mixers for thermal processing: a technical and historical perspective. AAPS PharmSciTech, 17(1), 3-19.

Miller, A. T., Safranski, D. L., Smith, K. E., Sycks, D. G., Guldberg, R. E., & Gall, K. (2017). Fatigue of injection molded and 3D printed polycarbonate urethane in solution. Polymer, 108, 121-134.

Rabinowicz, E., & Tanner, R. I. (1966). Friction and wear of materials. Journal of Applied Mechanics, 33(2), 479.

Rouf, S., Raina, A., Haq, M. I. U., Naveed, N., Jeganmohan, S., & Kichloo, A. F. (2022). 3D printed parts and mechanical properties: influencing parameters, sustainability aspects, global market scenario, challenges and applications. Advanced Industrial and Engineering Polymer Research, 5(3), 143-158.

Saini, P., Arora, M., & Kumar, M. R. (2016). Poly (lactic acid) blends in biomedical applications. Advanced Drug Delivery Reviews, 107, 47-59.

Sinha, S. K., & Briscoe, B. J. (2009). Polymer tribology. World Scientific.

Toh, H. W., Toong, D. W. Y., Ng, J. C. K., Ow, V., Lu, S., Tan, L. P., Wong, P. E. H., Venkatraman, S., Huang, Y., & Ang, H. Y. (2021). Polymer blends and polymer composites for cardiovascular implants. European Polymer Journal, 146, 110249.

Yu, L., Dean, K., & Li, L. (2006). Polymer blends and composites from renewable resources. Progress in polymer science, 31(6), 576-602.